

Electronic supplementary information

Understanding trends in methane oxidation to formaldehyde: statistical analysis of literature data and based hereon experiments

M. J. G. Fait, A. Ricci, M. Holena, J. Rabeah, M.-M. Pohl, D. Linke, E. V. Kondratenko*

Leibniz-Institut für Katalyse e.V., Albert-Einstein-Strasse 29a, 18059 Rostock, Germany

*Corresponding author: evgenii.kondratenko@catalysis.de

1 Powder X-ray diffraction

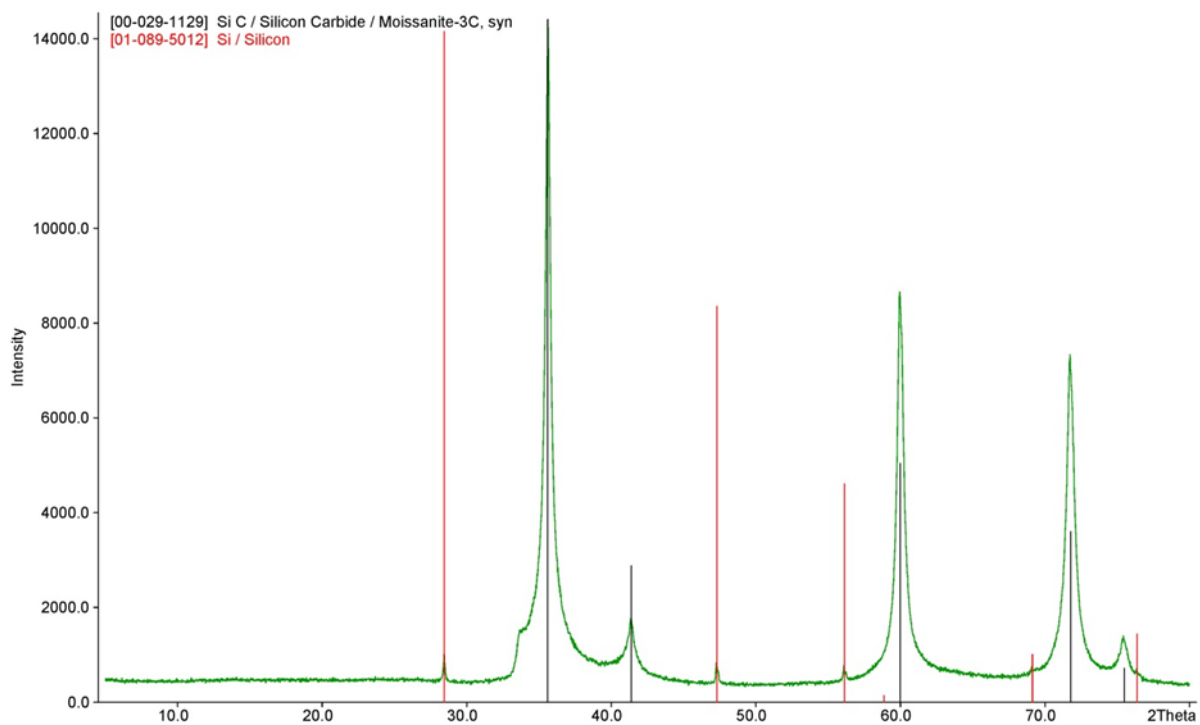


Fig. S1 Powder X-ray diffractogram of bare β -SiC and line diffractograms of reference phases β -SiC [00-029-1129] (black) and Si [01-089-5012] (red).

2 UV-vis diffuse reflectance spectroscopy

2.1 Experimental

UV-vis DR spectra of undiluted samples without pre-treatment were recorded under ambient conditions with reference to barium sulphate using a micro probe FCB-UV400-2 and a spectrometer AvaSpec-2048-2-USB-2 (both from Avaspec, The Netherlands). The spectra were converted into the Kubelka-Munk function ($F(R_\infty)$)¹

$$F(R_\infty) = (1 - R)^2/2R$$

where R is the reflectance.

2.2 Results

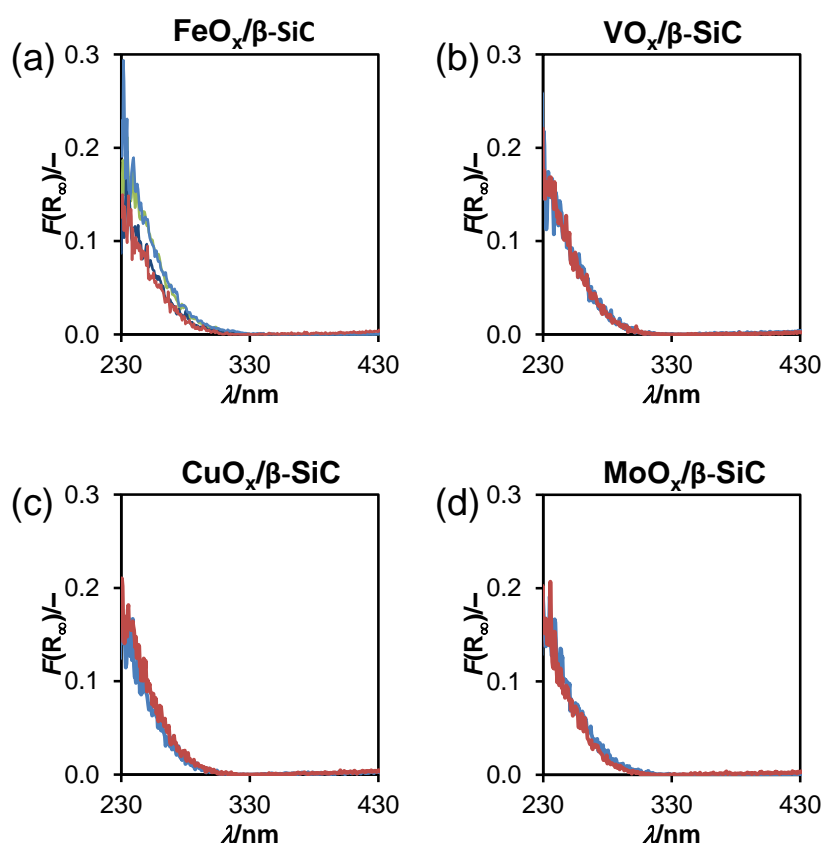


Fig. S2 UV-vis spectra of $MO_x/\beta\text{-SiC}$ samples ($M = \text{Fe}$ (a), V (b), Cu (c), Mo (d)) with different metal surface density (0.02 nm^{-2} , 0.15 nm^{-2} , 0.34 nm^{-2}). The spectrum of bare support $\beta\text{-SiC}$ is shown in (a).

The spectrum of the bare $\beta\text{-SiC}$ support (see Fig. S2(a)) does not significantly differ from the spectra of $MO_x/\beta\text{-SiC}$ regardless of the kind of metal and its loading. All spectra exhibited a continuous increase in absorption below 300 nm originated from C 2p electron transitions³ which is characteristic for $\beta\text{-SiC}$.⁴⁻⁶

To determine the band gap of $\beta\text{-SiC}$ for indirect transitions the square root of factor $F(R_\infty)$ (Kubelka-Munk function) and $h\nu$ (incident photon energy) was plotted against $h\nu$. The value of $h\nu$ extrapolated to $F(R_\infty) \cdot h\nu = 0$ gives an absorption energy which corresponds to the band gap, E_g .² The E_g values of $MO_x/\beta\text{-SiC}$ and $\beta\text{-SiC}$ samples amounted to 4.1 eV at room temperature independently of the metal and its site density. This value is in the range of literature data which are varying from 2.2 to 5.4 eV depending on the SiC polytype.^{3, 7}

3 EPR

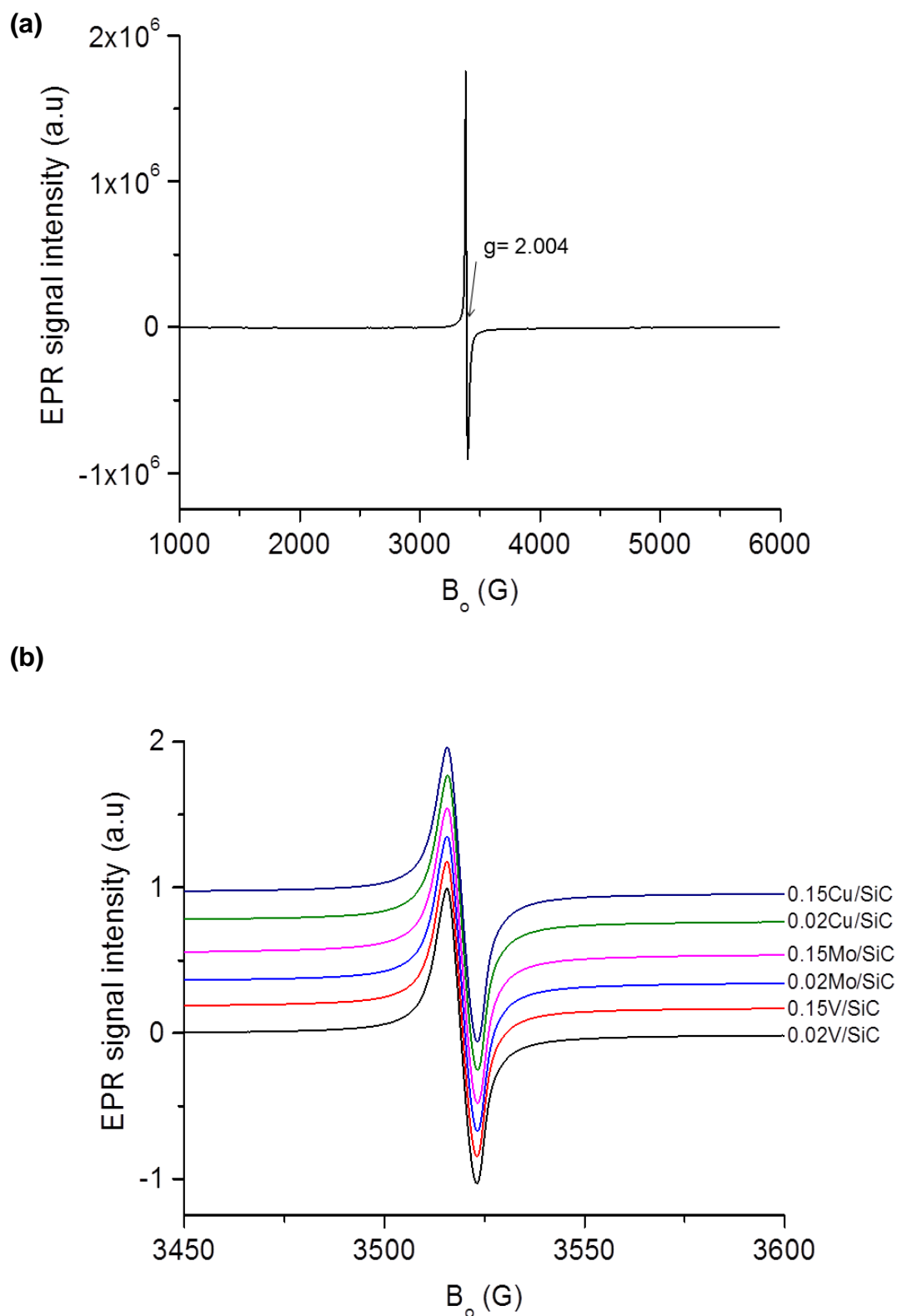


Fig. S3 EPR spectra of (a) bare β -SiC support measured at 100 K and (b) MO_x/SiC catalysts (VO_x , CuO_x , MoO_x with different surface density (0.02 and 0.15 nm^{-2})) measured at room temperature. The spectra were normalized to 1 for better comparison and show only EPR signal of β -SiC ($g = 2.004$).

4 Effect of metal and loading on S-X relationship at different temperatures

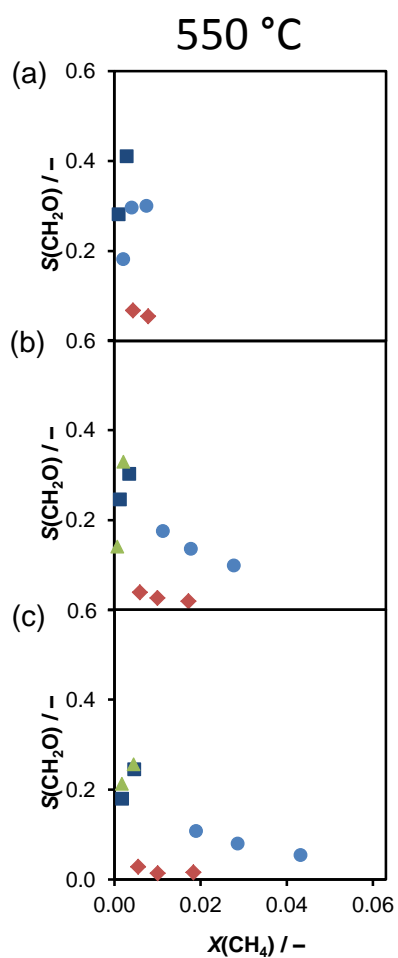


Fig. S4 Selectivity-conversion relationship for formaldehyde formed at 550 °C over $\text{MO}_x/\beta\text{-SiC}$ catalysts (VO_x , FeO_x , CuO_x , MoO_x) with different surface density (0.02 (a), 0.15 (b), 0.34 nm^{-2} (c)).

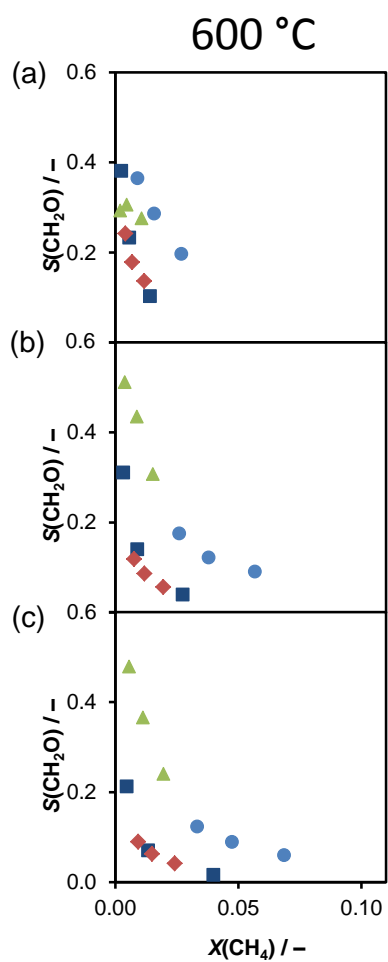


Fig. S5 Selectivity-conversion relationship for formaldehyde formed at 600 °C over $\text{MO}_x/\beta\text{-SiC}$ catalysts (VO_x , FeO_x , CuO_x , MoO_x) with different surface density (0.02 (a), 0.15 (b), 0.34 nm^{-2} (c)).

5 Arrhenius plots for methane conversion

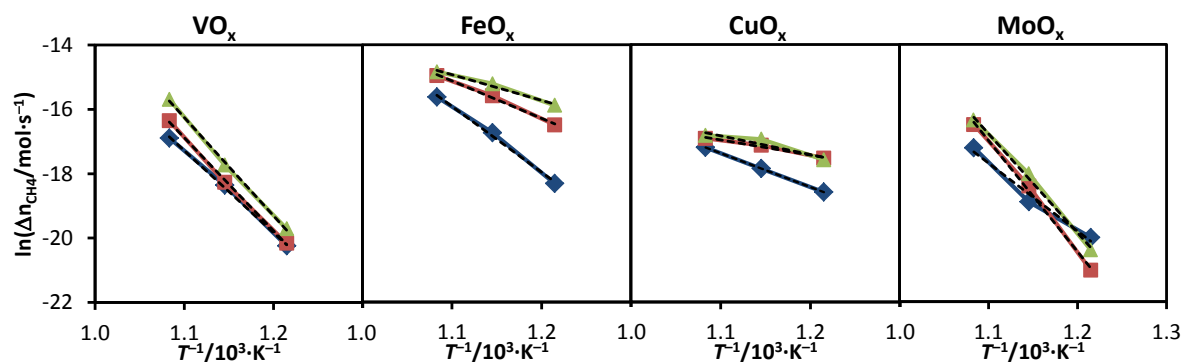


Fig. S6 Arrhenius plots of methane conversion over $\text{MO}_x/\beta\text{-SiC}$ catalysts (VO_x , FeO_x , CuO_x , MoO_x) with different metal surface density (0.02 (\blacklozenge), 0.15 (\blacksquare), 0.34 nm^{-2} (\blacktriangle)). Reaction conditions: $\text{CH}_4/\text{O}_2/\text{N}_2 = 30/10/60$, $\tau_{\text{mod}} = 0.9 \text{ g}\cdot\text{s}\cdot\text{ml}^{-1}$.

6 Activation energy of methane conversion vs. site density

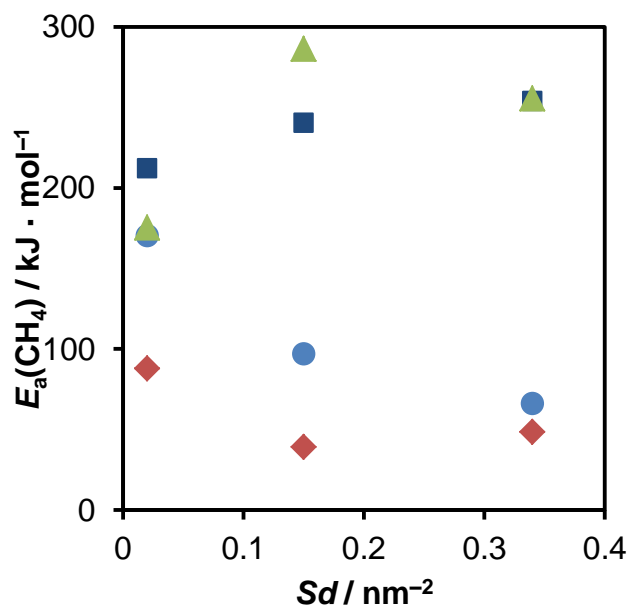


Fig. S7 Activation energy of methane conversion as a function of metal site density for $\text{MO}_x/\beta\text{-SiC}$ catalysts (V (\blacksquare), Fe (\bullet), Cu (\blacklozenge), Mo (\blacktriangle)).

7 Activation energy of formaldehyde formation vs. activation energy of methane conversion

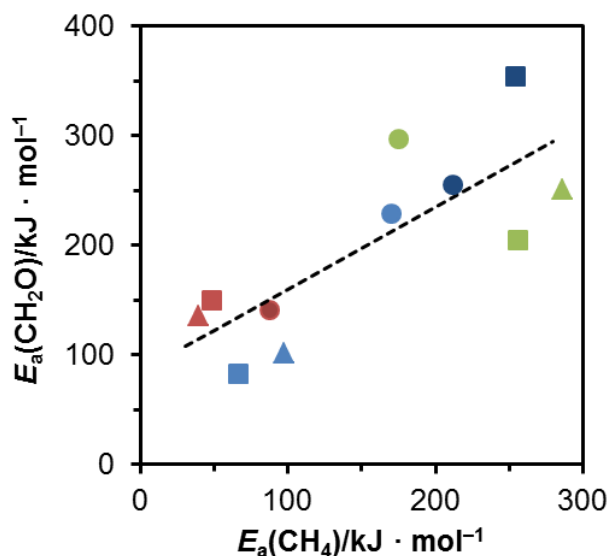


Fig. S8 Activation energies of CH_2O formation as a function of the activation energies of methane conversion for different site densities (0.02 (circles), 0.15 (triangles), 0.34 nm^{-2} (squares)) of $\text{MO}_x/\beta\text{-SiC}$ catalysts (VO_x , FeO_x , CuO_x , MoO_x).

8 Formaldehyde selectivity at 600 °C vs. activation energy of methane

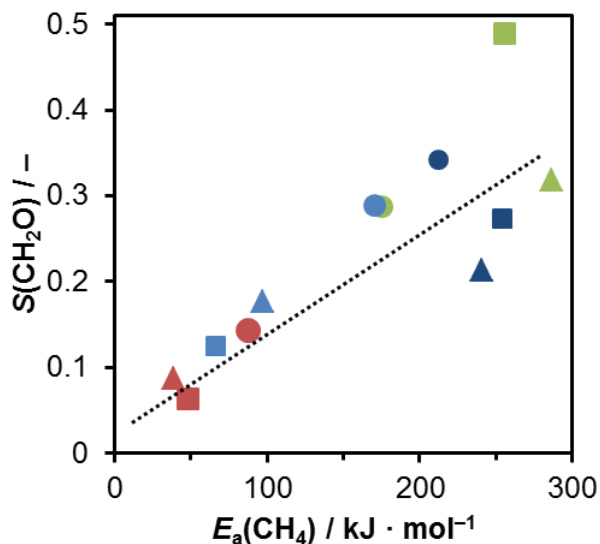


Fig. S9 Selectivity of CH_2O ($T = 600$ °C, $X(\text{CH}_4) = 0.015$) as a function of the apparent activation energy of methane conversion for different site densities (0.02 (circles), 0.15 (triangles), 0.34 nm^{-2} (squares)) of $\text{MO}_x/\beta\text{-SiC}$ catalysts (VO_x , FeO_x , CuO_x , MoO_x).

9 Formaldehyde selectivity at 550 and 600 °C vs. electronegativity of the active metal

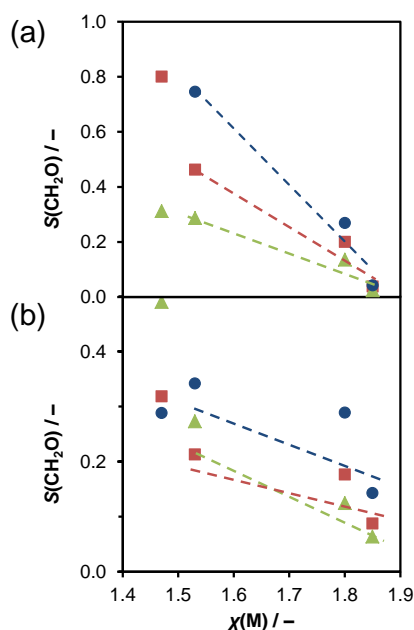


Fig. S10 Selectivity of CH₂O at 550 (a) and 600 °C (b) over MO_x/β-SiC catalysts (VO_x, FeO_x, CuO_x, MoO_x) with different metal surface density (0.02 (●), 0.15 (■), 0.34 nm⁻² (▲)) as a function of the metal electronegativity according to the Allen scale.

10 References

- 1 G. Kortüm, *Reflexionsspektroskopie*, Springer, Berlin, Heidelberg, New York, 1969.
- 2 S. P. Tandon and J. P. Gupta, *Phys. Status Solidi*, 1970, **38**, 363.
- 3 G.-Y. Feng, X.-Y. Fang, J.-J. Wang, Y. Zhou, R. Lu, J. Yuan and M.-S. Cao, *Phys. B (Amsterdam, Neth.)*, 2010, **405**, 2625.
- 4 P. Musumeci, R. Reitano, L. Calcagno, F. Roccaforte, A. Makhtari and M. G. Grimaldi, *Philos. Mag. B*, 1997, **76**, 323.
- 5 J. Chen, W. Tang, L. Xin and Q. Shi, *Appl. Phys. A: Mater. Sci. Process.*, 2011, **102**, 213.
- 6 J.-Y. Hao, Y.-Y. Wang, X.-L. Tong, G.-Q. Jin and X.-Y. Guo, *Int. J. Hydrogen Energy*, 2012, **37**, 15038.
- 7 S. Lazanu, I. Lazanu, E. Borchini and M. Bruzzi, *Nucl. Instrum. Methods Phys. Res., Sect. A*, 2002, **485**, 768.